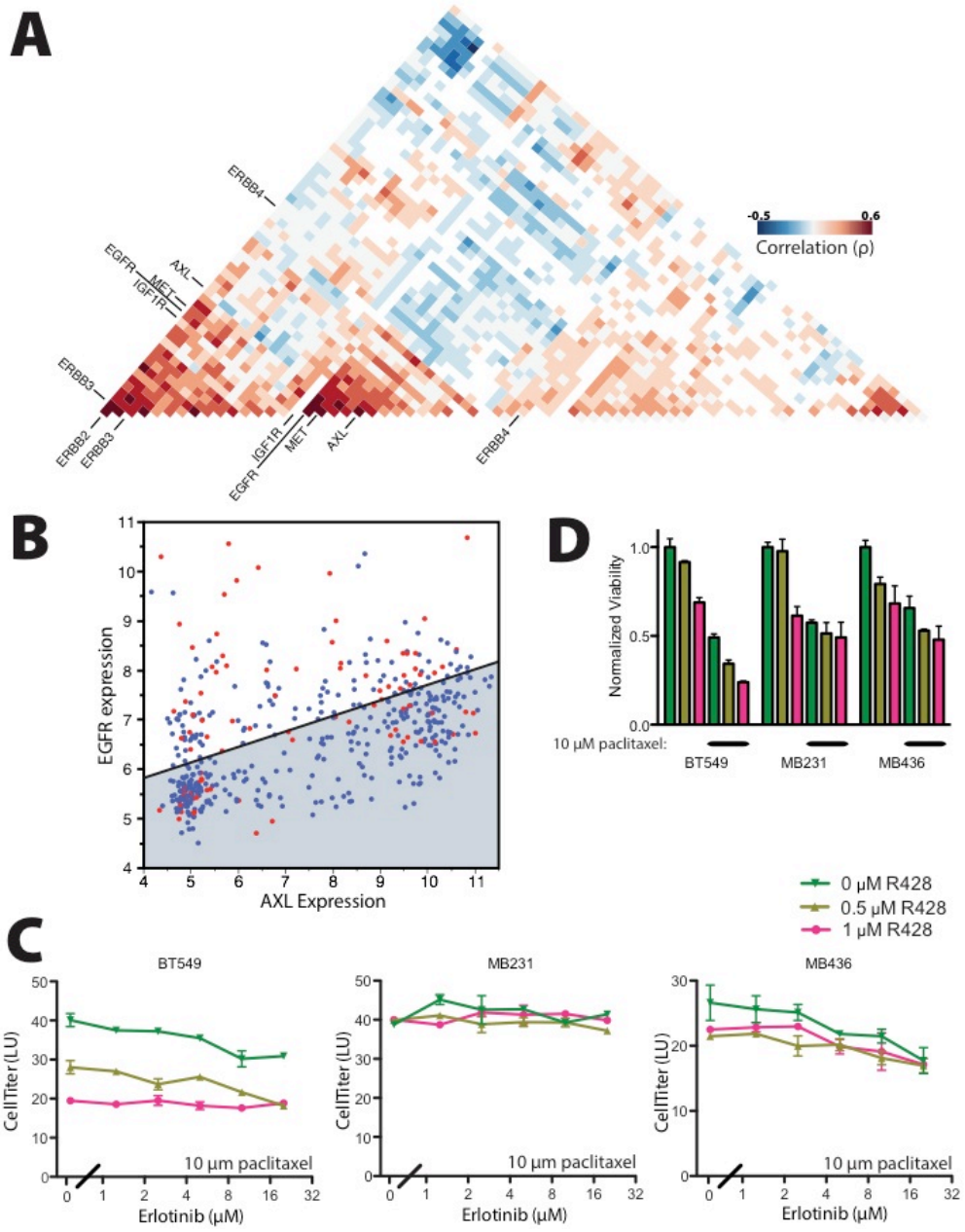

Fig. S1. Support vector classification to identify mechanisms of drug resistance. A) Spearman correlations for all pairs of GO-annotated receptor tyrosine kinases across all cell lines within the CCLE. Receptors were ordered by hierarchical clustering using Spearman correlation as a distance metric and average linkage. Roughly three or four clusters emerge of RTKs with highly correlated expression. Only significant correlations ($p < 0.01$) are shown. B) Classifier for erlotinib sensitivity based on AXL and EGFR expression. Blue dots indicate resistant cell lines, and red dots sensitive cell lines. The blue region indicates the region for which the classifier predicts cells to be resistant. Axes are RMA-normalized probe values. C) Dose response surfaces for R428 and erlotinib with 10 μM paclitaxel in three triple negative breast carcinoma cell lines with overexpression of EGFR and AXL. D) Viability measurements for varying amounts of R428 with or without paclitaxel. Error bars indicate standard error of biological triplicates.

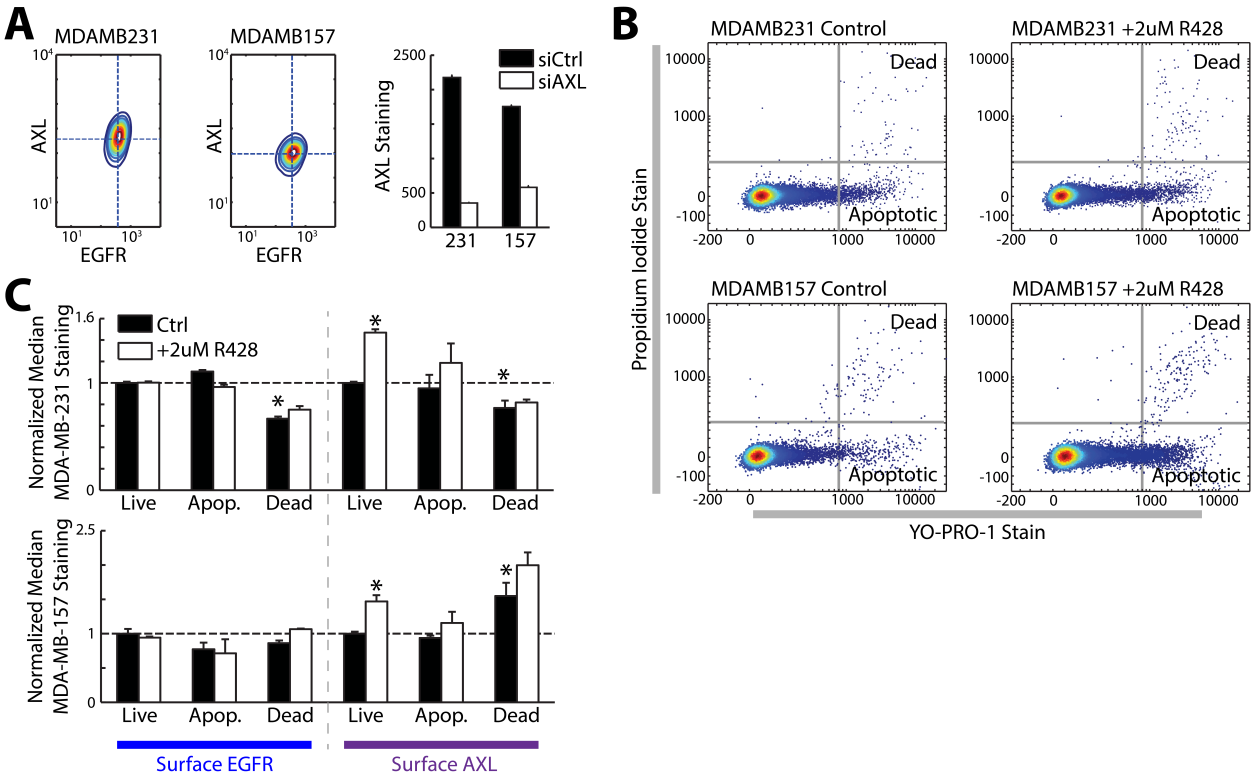

Fig. S2. Single-cell EGFR and AXL expression with R428 treatment. A) Live-cell immunostaining of cell lines under basal conditions to measure surface EGFR and AXL abundance. Colors and lines indicate population distribution, with warmer colors denoting higher density. Dashed lines denote median expression across the population. AXL live-cell immunostaining specificity was confirmed by AXL siRNA treatment. B) Measurement of apoptosis and cell death in response to R428 treatment. 20,000 cells are shown within each plot. C) EGFR and AXL surface levels measured by live-cell immunostaining for each of the subpopulations shown in B, following 24 h treatment with 2 uM R428 (*$p<0.05$, Student's t-test comparison to live untreated cells, biological triplicate).

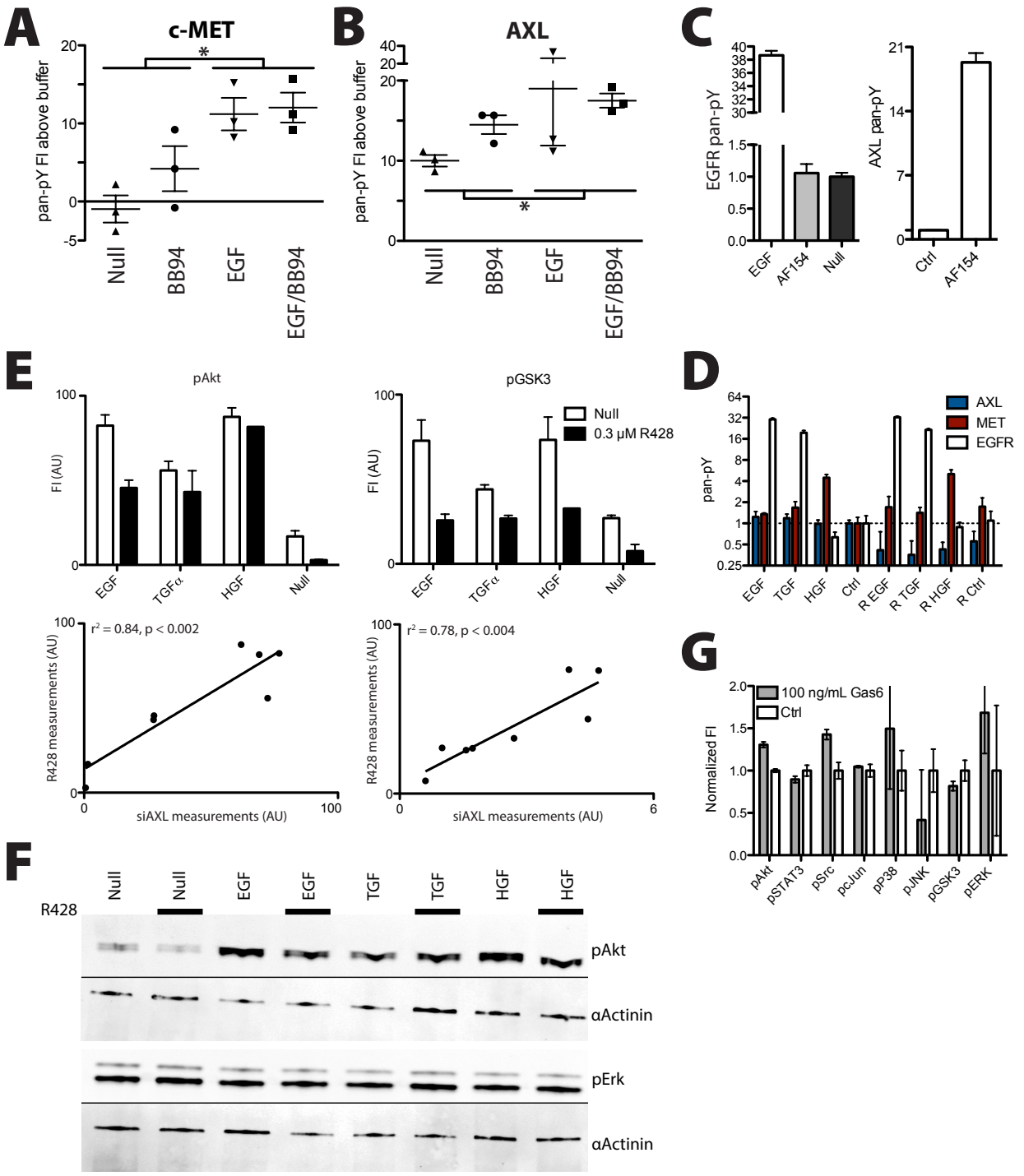

Fig. S3. RTK crosstalk occurs in triple negative breast carcinoma cells. Activation of Met (A) and AXL (B) in the presence of batimastat (*$p < 0.05$, paired Student's test). C) Measurement of receptor activation upon treatment with an activating antibody for the AXL receptor. D) Receptor activation measurement for conditions corresponding to those of downstream analysis. E) Inhibition of AXL kinase activity with 0.3 μM R428 and comparison to knockdown of the receptor. Akt and GSK3 measurements upon stimulation of MDA-MB-231 cells (top) and correlation with siAXL measurements (bottom). Pearson correlation values and significance is

shown. For ELISA measurements, error bars indicate standard error of biological triplicate measurements. F) Western blot validation of a subset of phosphosite measurements. Results are qualitatively identical to those performed by ELISA. G) Downstream signaling measured after 5 min of 100 ng/mL Gas6 stimulation.

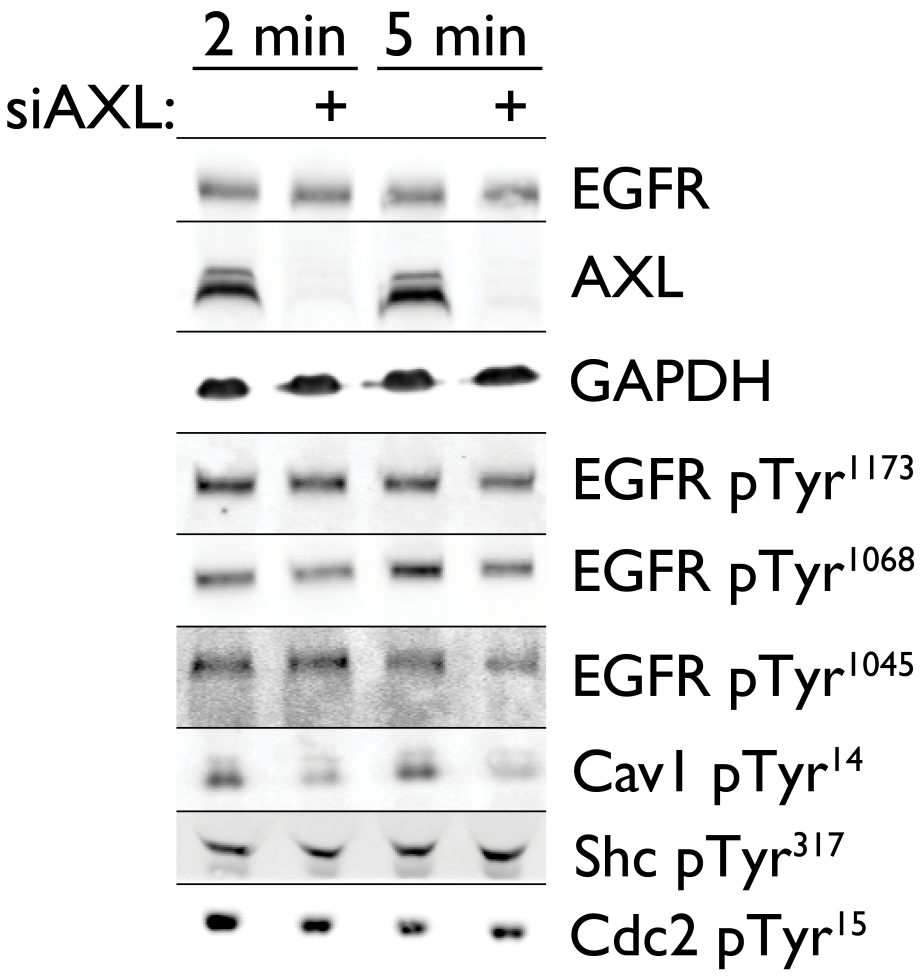

Fig. S4. Receptor activation is similar in AXL knockdown cells. Cells were starved for 4 hr and stimulated with 100 ng/mL EGF for the time indicated. Only caveolin pTyr^{14} was substantially changed by AXL knockdown. Blots are representative of two experiments.

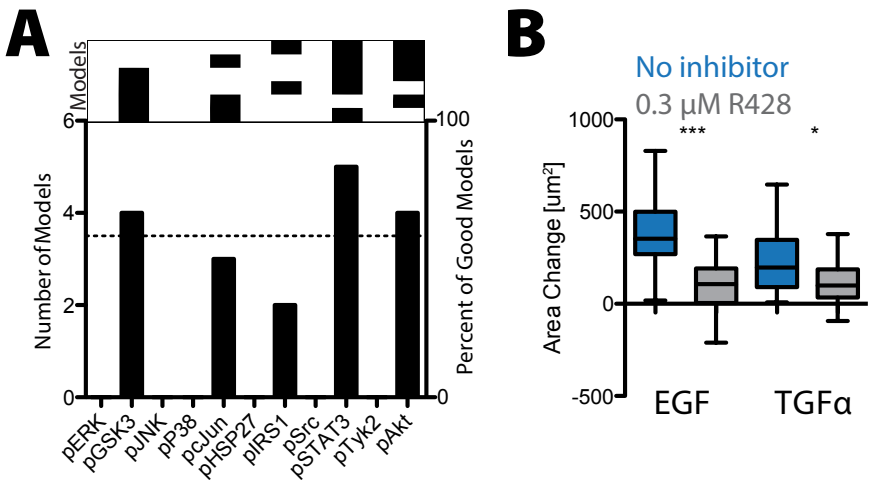

Fig. S5. AXL signaling is required for EGF elicited protrusion. A) Variable enrichment upon PLSR model reduction. Each sufficiently predictive model (Q2 > 0.6) of the wild-type protrusion measurements is shown (top). Bars indicate the frequency with which variables are included in the six selected reduced models. The dotted line indicates the threshold of significant enrichment ($p < 0.05$, hypergeometric test). B) MDA-MB-231 cells treated with EGF or TGFα and R428. R428 also has an effect on TGFα-elicited protrusion, perhaps less than EGF as predicted (***$p < 0.001$, *$p < 0.05$, Mann-Whitney test). Single cells were pooled from three independent experiments (***$p < 0.001$, *$p < 0.05$, Mann-Whitney test, N=30-36).

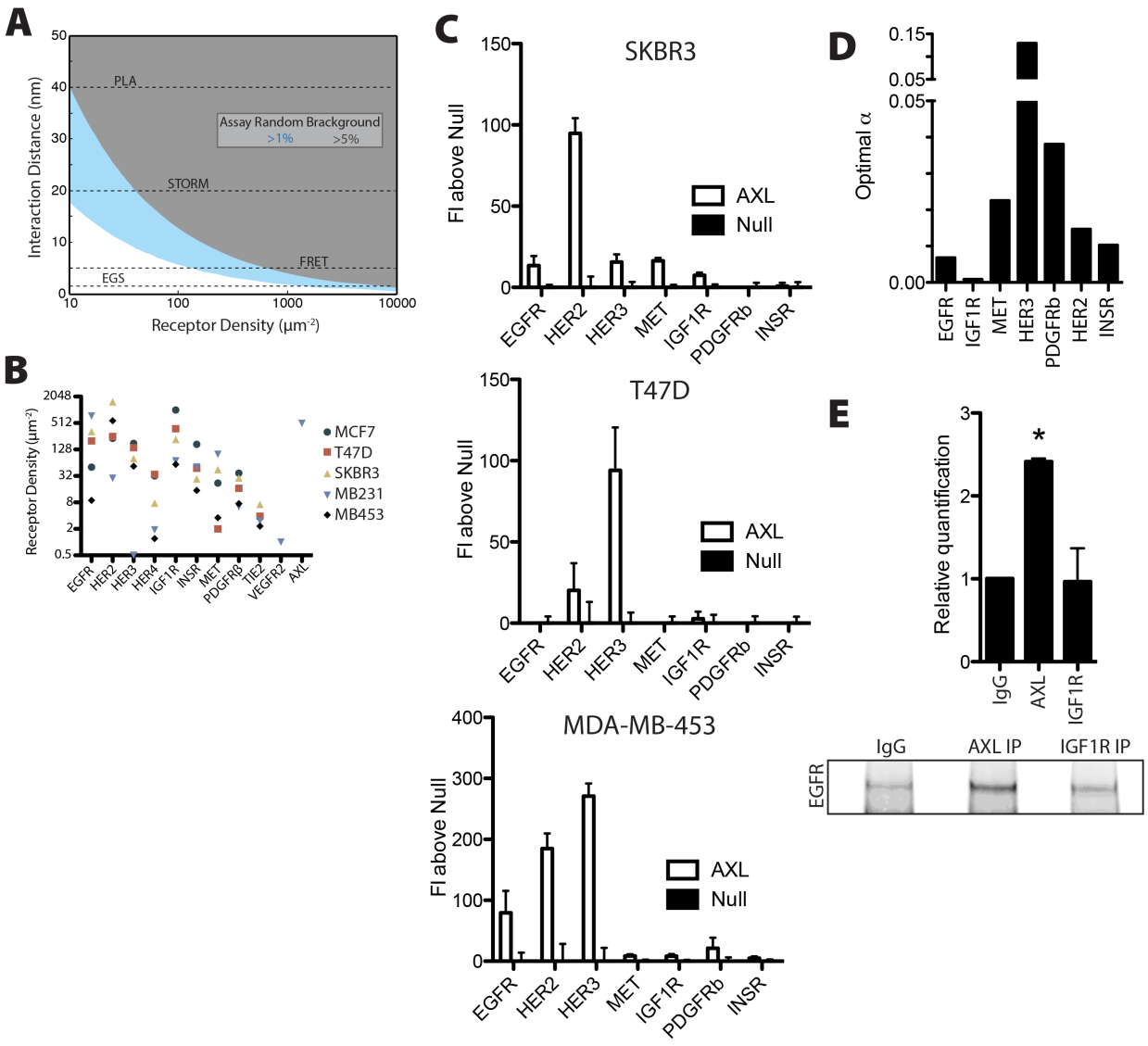

Fig. S6. A multivariate chemical crosslinking approach to study receptor colocalization. A) A random receptor distribution model eliminates antibody-based in situ methods as means to study co-clustering of surface receptors at high expression. Each colored region indicates a threshold of background for a particular assay with characteristic distance and receptor density. B) Absolute quantification of receptor expression identifies which receptors can be analyzed using various methods. Details of receptor density quantification are given in the Methods. Points not shown are below the limit of detection (< 2 μm^{-2} for every receptor). C) Quantification of AXL crosslinking in three luminal/HER2+ breast carcinoma cell lines. For each, overexpression of AXL is compared to cells with no overexpression, as AXL is not expressed in these cells (N=6 replicates). D) Optimal α_i parameters for the data across seven RTKs. E) Reciprocal co-immunoprecipitation of EGFR with AXL or IGF1R. A blot of the immunoprecipitation is shown (bottom) along with quantification of duplicate experiments (top, *$p < 0.02$, Student's test).

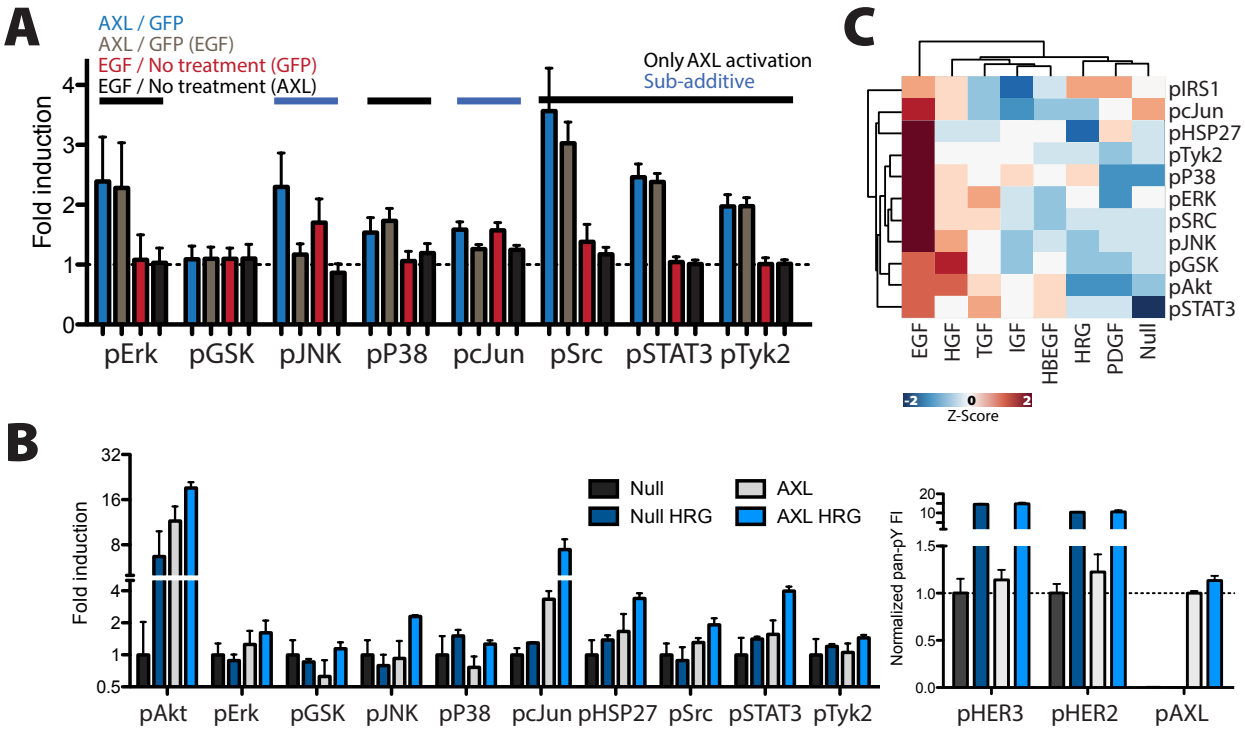

Fig. S7. Crosslinking can predict receptor transactivation pairs. A) AXL expression does not result in EGF-transactivated signaling in MCF7 cells. Each bar indicates the ratio of two treatment conditions, with the standard error propagated from the error of each individual measurement (biological triplicate measurements). Synergy in signaling response would correspond to a greater black than red bar for a given phosphosite. B) Signaling measurement of AXL-transfected MDA-MB-453 cells stimulated with HRG for 5 min. Error bars indicate standard error of biological triplicate measurements. C) Signaling measurement of phosphosites across different growth factors for use in Fig. 7B. MDA-MB-231 cells were lysed after 5 min stimulation with each growth factor. Each phosphosite was mean centered and variance normalized.

Receptor	Erlotinib Synergy	Lapatinib Synergy
AXL	$p < 0.001$	$p < 0.001$
EPHA1	$p < 0.001$	$p < 0.001$
FGFR1	$p < 0.001$	$p < 0.001$
MST1R	$p < 0.05$	$p < 0.05$
EPHA2	$p < 0.05$	$p < 0.05$
ERBB3	$p < 0.05$	$p < 0.05$

Table S1. RTK genes significantly associated with both erlotinib and lapatinib resistance. Significance is calculated by randomized controls.

	Unstim	EGF	TGF	HGF	Paired
pErk		•	•		•
pGSK3	•	•	•	•	•
pJNK					
pP38					
pcJun		•	•		•
pHSP27	•				
pIRS1			•		•
pSrc					
pSTAT3					
pTyk2					•
pAkt	•				

Table S2. Individual comparisons were made between conditions with AXL-targeting or nontargeting siRNA using a Student's t-test. Paired comparisons were made by a signed rank test. (*$p < 0.05$).

Model	AIC	AIC Relative Likelihood	AICc	AICc Relative Likelihood
1	277	10^{-4}	277	0.0005
2	266	**0.58**	269	**1.0**
3	305	10^{-17}	307	10^{-16}
4	279	10^{-5}	284	10^{-6}
5	268	**0.10**	273	0.025
6	274	0.0002	277	0.0004
7	302	10^{-16}	305	10^{-15}
8	265	**1.0**	270	**0.25**

Table S3. Relative model goodness of fits based on the Akaike information criterion. Models 2 and 8 cannot be distinguished in their goodness of fit, but have similar biological conclusions.